This article has been accepted for publication in a future issue of this journal, but has not been fully edited. Content may change prior to final publication. Citation information: DOI 10.1109/TMECH.2017.2654446, IEEE/ASME Transactions on Mechatronics

Robust and Inexpensive 6-Axis Force-Torque Sensors using MEMS Barometers

Jacob W. Guggenheim, *Student Member, IEEE,* Leif P. Jentoft, *Student Member, IEEE,* Yaroslav Tenzer, *Member, IEEE,* and Robert. D. Howe, *Fellow, IEEE*

***Abstract*—Current commercial force-torque sensors are sensitive and accurate, but are also typically expensive and fragile. These features limit their use in cost-sensitive applications and unstructured environments such as people's homes. This paper presents a new design for an inexpensive and robust force-torque sensor that uses MEMS barometer transducers. The new design results in a six-axis force-torque sensor with an R^2 greater than 0.90 for $\mathbf{F}_x$ and $\mathbf{F}_y$ and an R^2 greater than 0.98 for $\mathbf{F}_z$, $\mathbf{M}_x$, $\mathbf{M}_y$, and $\mathbf{M}_z$ during compound loading. Furthermore, this sensor can be assembled in two days with off-the-shelf components for less than twenty dollars.**

I. Introduction

FORCE-TORQUE sensors find wide application in industry where they are used for robotic assembly, grinding and polishing, and testing rigs. They are also used for research in rehabilitation devices, haptics, telepresence, robotic manipulation, and cell biology [1]. While a variety of transduction approaches have been used to create force-torque sensors, strain gauges are the most popular. They are accurate, small, and easily configured to measure multidimensional strains. They are, however, difficult to bond, and require complicated overload protection. The signals produced are typically small, requiring careful shielding and amplification [2]. This leads to a complex and expensive fabrication process. Piezoelectric transducers are also widely used, but they lack steady-state response so they are typically restricted to dynamic loads [3]. Niche applications use more exotic technologies such as Fiber-Bragg gratings (which measure frequency-shift in light transmitted along an optical fiber) [4], [5] and integrated MEMS transducers for micromanipulation [6], [7], [8]. To date, most multi-axis force-torque sensors are expensive and are susceptible to overload damage.

A number of low-cost force sensor technologies have been developed but they have significant performance limitations. Thick-film piezoresistive transducers, such as Force-Sensitive Resistors (FSRs), have a highly nonlinear response and require a bias force that can be difficult to regulate. Rikkers et al. [9] ultimately concluded that FSRs are better suited for qualitative measurements rather than precise quantitative measurements. Compliant devices that measure displacement, such as the SpaceMouse [10], [11], rely on significant displacements that exclude applications like robotic manipulation where high resonant frequencies and positioning accuracy are important. Many new applications, particularly for robotic manipulation in human environments would be possible with the availability of low-cost, multiaxis sensors that are robust to impacts and other excess loading events.

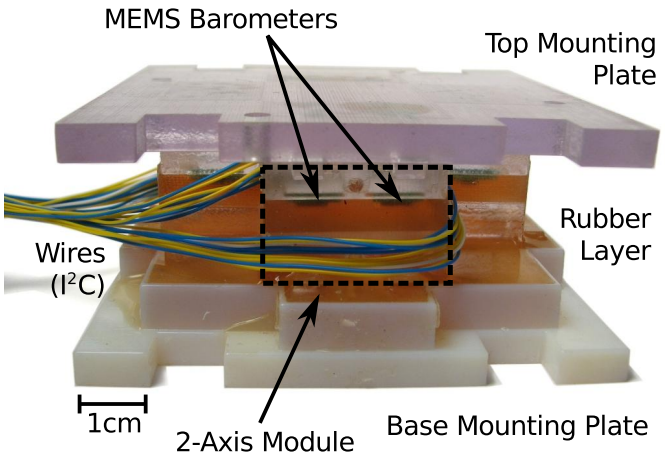

Fig. 1. MEMS Barometers can be used to create a six-axis force-torque sensor that is inexpensive and robust. The prototype consists of two rigid plates joined by four modules consisting of rubber blocks with MEMS barometers embedded inside. Signals are transmitted digitally to logging software.

In this paper, we present a method for fabricating low-cost, robust force-torque sensors using MEMS barometer chips. Recent work has shown that MEMS barometers may be modified to serve as tactile sensors with excellent sensitivity (<0.01 N), linearity (< 1%), and bandwidth (>100 Hz) [12], [13]. These air pressure sensors are mass produced for consumer applications so they provide excellent performance at minimal cost. By casting them in rubber and arranging them in appropriate configurations, they can be converted to measure forces and torques. We begin by presenting the sensor design and fabrication process. Next, we give an analysis that relates design parameters to sensor response. The following section evaluates a prototype sensor to demonstrate performance. Finally, the advantages and limitations of the sensor are discussed in the context of other approaches.

II. Design and Analysis

A. Transducers

Barometric sensor chips have been developed for various applications including vertical positioning augmentation for

Jacob Guggenheim is with Massachuestts Institute of Technology
Leif P. Jentoft, Yaroslav Tenzer, and Robert D. Howe are with the Harvard School of Engineering and Applied Science. Email ljentoft@seas.harvard.edu
Leif P. Jentoft and Yaroslav Tenzer are also founders at TakkTile LLC
Manuscript received Jun 24 , 2016

This article has been accepted for publication in a future issue of this journal, but has not been fully edited. Content may change prior to final publication. Citation information: DOI 10.1109/TMECH.2017.2654446, IEEE/ASME Transactions on Mechatronics

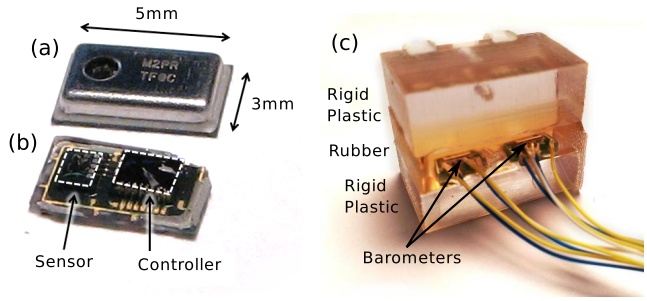

Fig. 2. The MEMS barometer used in the design of the force torque sensor bare (left), and cast into a 2-sensor module (right).

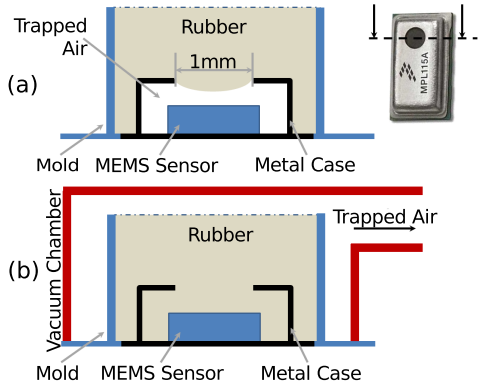

Fig. 3. The rubber casting process of the MEMS barometer sensor. (a) Air bubble is trapped inside the MEMS barometer when one is cast in rubber. (b) Vacuum degassing eliminates air bubbles allowing the casing to be filled with rubber.

GPS systems and personal weather stations. As they are increasingly integrated into smart phones, these sensors are mass produced at low cost, with low power consumption and minimal package size. While several versions are available, all of them use a MEMS transducer along with integrated signal conditioning, analog-to-digital conversion, and bus interface in a standard surface mount package. Because of the need to detect small changes in atmospheric pressure that correspond to changes in elevation, these sensors have excellent sensitivity. Because the signal output for these sensors is digital, signal-to-noise is excellent and interfacing is easy. Previous work has shown that casting these sensors in rubber and vacuum-degassing the units to remove air bubbles provides a means of transmitting an applied surface force to the sensing diaphragm inside the sensor package (Fig. 3) [12]. The MEMS barometer chip selected for the prototypes presented here is the MPL115A2 (Freescale Semiconductor Inc., Austin, TX, USA). It was selected because of its small size (5 x 3 x 1.2 mm), low cost, and the provision of a large ventilation hole located directly above the MEMS pressure sensor (Fig. 1).

B. Design

The proposed design uses the standard package configuration for force-torque sensors for end-of-arm robotics applications, i.e. a pair of mounting plates separated by a relatively thin internal structure that houses the transducers. The central challenge in force sensor design is to find a spatial configuration for the internal structure so that the transducers provide good signals in response to the full range of anticipated loads applied to the plates. Additional design goals include minimized fabrication costs and the ability to withstand overloads due to impacts. One attractive approach is to configure the structure as a set of modules, each consisting of a rubber block with two embedded transducers. This simplifies construction and minimizes cost, and allows easy analysis and visualization of the mechanical function of the resulting sensor. In each module, the barometer chips are first molded at the bottom of a rubber block (Fig. 4). The blocks are then arranged between the sensor mounting plates. Four modules are used in the current implementation for symmetry, although a trilateral design could also work.

C. Analysis

The rubber-encased MEMS barometers measure normal stress in the direction normal to the chip package, with insignificant response to normal stresses in the lateral direction or to shear stresses. Given the spatial configuration of the modules and their transducers, a mechanical analysis can relate the forces and torques applied to the mounting plates to local loads on the transducers, in terms of the geometric design parameters. To relate the local normal stress to the applied load, four loading cases must be examined: normal force in the z direction, lateral force along the x- (or y-) axis, moment around the z-axis, and moment around the x- (or y-) axis.

Forces and moments applied to the mounting plates are transmitted to the four modules as shown in Fig. 4. A pure normal load F_z (Fig. 4c) results in equal uniaxial compression of the four modules, so

$$\sigma_z = \frac{F_z}{4LW} \tag{1}$$

where σ_z is the normal stress on the transducer, F_z is the normal force, W is the width of each rubber module as shown in Fig. 4, and L is the length. The sensitivity of the sensor to loads along the z-axis, S_{F_z}, is then

$$S_{F_z} = \frac{KF_z}{4LW} \tag{2}$$

where K is a calibration constant with units of sensor counts per unit stress. Thus, increasing the area of the rubber increases the range of F_z that can be measured before the transducer saturates and decreases the sensitivity. It is important to note that K also takes into account the effects of the material properties of the rubber being used. A pure moment around the x-axis results in tension of sensors located on the positive side of the x-axis, and compression on the sensors on the negative side as shown in Fig. 4d. Modeling the combination of modules as a short beam with the cross-section shown in Fig. 4a, loaded in pure moment, yields an expression for S_{M_x}, the sensitivity to applied moments around the x-axis.

$$S_{M_x} = \frac{KM_x y_i}{2\frac{LW^3}{12} + 2(\frac{L^3W}{12} + r^2LW)} \tag{3}$$

This article has been accepted for publication in a future issue of this journal, but has not been fully edited. Content may change prior to final publication. Citation information: DOI 10.1109/TMECH.2017.2654446, IEEE/ASME Transactions on Mechatronics

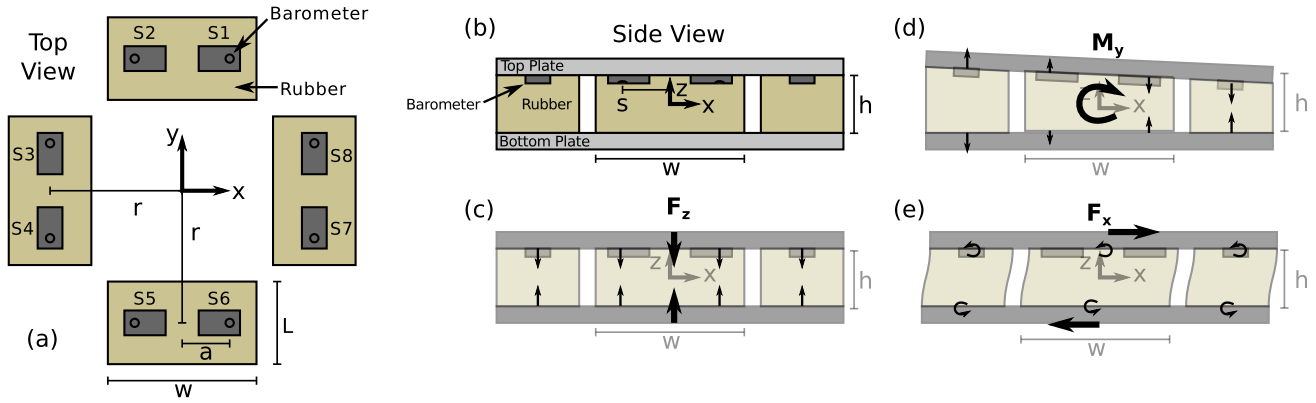

Fig. 4. Design parameters of sensor using four modules. Coordinate origin located at center of sensor in each direction. (a) Top and (b) side views of the assembled sensor. (c) Deformation of the sensor as a result of applied normal force. (d) Deformation of the sensor as a result of the applied moment. (e) Deformation of the sensor as a result of shear force.

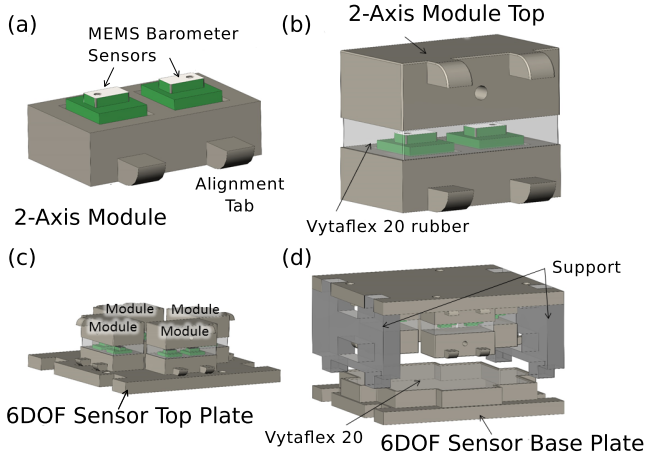

Fig. 5. The fabrication of the 6DOF sensor begins with casting four 2-axis modules. Each module contains two Fig.3.(a) Single-axis module base with MEMS barometers glued on with cyanoacrylate. Tabs on the side are used to align module in mold. (b) Complete single-axis module. (c) Four single-axis modules placed symmetrically on base-plate of 6DOF force torque sensor. (d) Bottom assembly as it is being attached to the top-plate. The top of the single-axis modules will slightly submerge into the curing Vytaflex-20, thus securing on the top-plate upon curing of the poly-urethane rubber.

where K is the calibration constant with units sensor counts per unit stress, M_x is the applied moment around the x-axis, y_i is the distance from the sensor to the x-axis, with $y_i = a$ for the modules lying on the x-axis and $y_i = r$ for the units on the x-axis. y_i, and thus a and r, can be used to modify moment response independent of normal load response. Due to symmetry, moments around the y-axis take the same form.

A shear load F_x, on the top and bottom of the rubber block causes a moment around the center proportional to the height of the rubber h as shown in Fig. 4e. This is balanced by a moment at the end of each rubber block. This becomes a standard beam-bending problem. Although the beams are short and thus shear plays a role in their deflection, the transducers measure only axial load so the normal bending equations apply. The sensitivity to applied shear loads along the x-axis, S_{F_x}, is then

$$S_{F_x} = \frac{KF_x h x_i}{2\frac{L^3 W}{12} + 2(\frac{LW^3}{12} + r^2 LW)} \tag{4}$$

where K is the calibration constant, F_x is the shear load, h is the height of the rubber block, and x_i is the distance between the sensor and the y-axis of the beam. Thus, the higher the rubber block (and the closer the sensor units to the edge) the stronger the shear force response. Due to symmetry, a similar form applies for shear loads in the y-direction. Finally, a moment around the z-axis results in shear loads on each of the blocks. The sensitivity to applied moments around the z-axis, S_{M_z}, is then

$$S_{M_z} = \frac{KK_g M_z h a}{4\frac{W^3 L}{12}} \tag{5}$$

where M_z is the moment applied around the z-axis and h, a, K, K_g, W, and L are as previously defined. Because these shear loads are not perfectly oriented along the long axis of each block, we can include an additional geometric constant K_g to account for the slight change in the second moment of area. If we assume that the stresses are superimposable, the total response takes the form $F = US$, where

$$F = \begin{bmatrix} F_x \\ F_y \\ F_z \\ M_x \\ M_y \\ M_z \end{bmatrix} \quad S = \begin{bmatrix} S_1 \\ S_2 \\ S_3 \\ S_4 \\ S_5 \\ S_6 \\ S_7 \\ S_8 \end{bmatrix} \tag{6}$$

$$U = \begin{bmatrix} A & -A & -A & -A & -A & A & A & A \\ A & A & A & -A & -A & -A & -A & A \\ B & B & B & B & B & B & B & B \\ -C & -C & -C & C & C & C & C & -C \\ C & -C & -C & -C & -C & C & C & C \\ -D & D & -D & D & -D & D & -D & D \end{bmatrix}$$

In matrix U, A, B, C, and D are the collected constants from equations 4, 2, 3, and 5, respectively. Note that this matrix is rank-6, and that each constant is independently tunable via

This article has been accepted for publication in a future issue of this journal, but has not been fully edited. Content may change prior to final publication. Citation information: DOI 10.1109/TMECH.2017.2654446, IEEE/ASME Transactions on Mechatronics

dimensions W, L, h, r, and a. These equations directly relate each of the design parameters to the sensor output, and can be used to optimize the configuration for a desired sensitivity and range. The final 6-axis response can then be calibrated using a standard least-squares fit to experimental data. An affine term is added to compensate for a fixed offset in the sensor readings.

D. Fabrication

The barometer sensors (MPL115A2, Freescale Semiconductor) are mounted on custom PCBs (TakkStrip, TakkTile LLC, Cambridge MA, USA). These PCBs are glued with cyanoacrylate onto a rapid prototyped (RP) plastic bottom plate printed from VeroBlue (Stratasys Ltd, USA). They are placed symmetrically and the ventilation hole is oriented outwardly as shown in Figure 3a. The distance between the centers of the two ventilation holes is $2a$ = 13.5mm. A top piece, also RP plastic measuring W = 25mm by L = 15mm by 9mm in height, is held in place h = 3mm above the top of the bottom RP plastic plate, again measuring 25mm by 15mm but with a height of 7mm. Urethane rubber (Vytaflex20, Smooth-On, Inc., Easton, USA) is then poured over the entire assembly filling the space in between the top and bottom plate. Figure 3b shows the cured assembly for the two-axis module. As in [12], the module is placed in a vacuum chamber immediately after the rubber is poured to pull the rubber into the MEMS sensor hole, thus eliminating any air bubbles that may be trapped within the barometer case. This 2-axis module is capable of sensing force both in the normal direction and the shear direction (defined to be perpendicular to the short edge of the sensor). Four of these two-axis modules are then placed symmetrically around a 3D printed resin bottom plate and fixed with cyanoacrylate as illustrated in Fig. 5. The distance between the long edge two-axis modules and the parallel edge of the bottom plate is 9.25mm while the distance from the short edge of the two-axis modules to the parallel edge of the plate is 24.9mm. r = 20.55mm. The entire bottom plate measures 75mm by 75mm by 5mm in height. From here a top plate, also measuring 75mm by 75mm but with a height of 11.5mm, is held in place by two supports thus ensuring that the top and bottom plates are parallel and leaving the total height of the sensor at 30mm as shown in Fig. 5. The space between the top plate and the top of the single-axis modules is filled with Vytaflex 20. This is done to ensure that no internal stresses are placed on the MEMS barometric sensors by any minor variations in module height. Fabrication of the sensor can be completed in two days with the majority of the time dedicated to letting the rubber cure.

E. Thermal Behavior

An important characteristic to investigate when choosing a rubber for casting is how the rubber responds to temperature. Although the barometers provide an integrated temperature sensor for thermal compensation, the factory calibration values are set for the sensors behavior under air rather than rubber. Due to differences in the thermal expansion coefficients of the silicon diaphragm, the rubber, and the metal case, the choice of rubber also affects the behavior. Two polyurethane rubbers

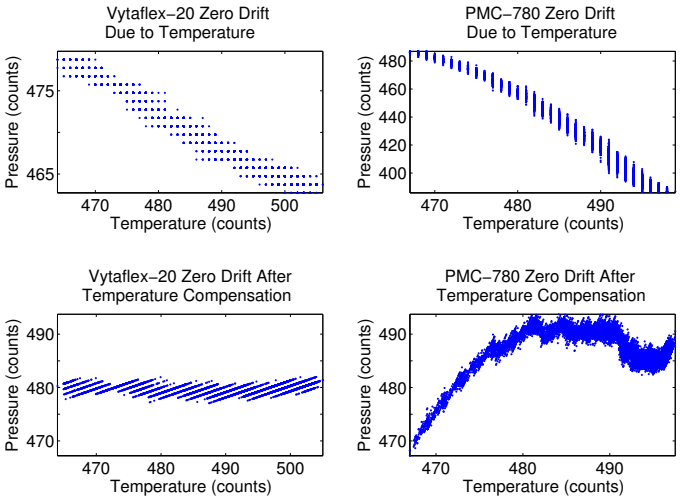

Fig. 6. Under zero load, changes in temperature cause the sensor response to drift under (a) Vytaflex-20 and (b) PMC-780. The results of applying a linear temperature compensation on data taken under zero loading are shown for (c) Vytaflex 20 and (d) PMC-780.

were chosen for comparison. Figure 6a and 6b show plots of Vytaflex 20 and PMC-780 (Smooth-On, Inc., Easton, USA) responses to temperature respectively. Each rubber was cast over a sensor, vacuum-degassed, and allowed to cure. To test the temperature drift, the sensors were warmed under a heat lamp and then allowed to coolback to room temperature at constant pressure. The data in Fig. 6a and 6b represent the response of the rubber-casted sensors close to room temperature. Although both rubbers are affected by the temperature, the MEMS sensor cast in PMC-780 responds more strongly and less linearly. Figure 6c and 6d show the result of applying a linear temperature compensation algorithm.Vytaflex 20 was used for the full force-torque sensor on the basis of this superior performance. All of the subsequent trials for the 6DOF force-torque sensor in this paper were conducted at constant temperature and therefore no temperature compensation was applied.

F. Robustness

Most force-torque sensors use strain gauges placed precisely along with a series of complicated flexures to help decouple the different force axes. It is critical to protect these components from overloading. As a result many force-torque sensors are larger and heavier than they need to be for their application. Because our sensor design does not rely on complicated flexures and fragile strain gauges, the sensor does not require any excess components whose sole purpose is support. This simultaneously allows the sensor to be compact, to have a low mass, and to be simple to fabricate. Despite this though, the sensor is still very robust. As demonstrated in [12], the MEMS barometric sensor, once cast in rubber, is robust enough to withstand high loads and impacts, such as a hammer blow.

III. Methods and Results

The sensor was calibrated and tested by securing it to a calibrated commercial 6-axis force-torque sensor (Gamma Force

This article has been accepted for publication in a future issue of this journal, but has not been fully edited. Content may change prior to final publication. Citation information: DOI 10.1109/TMECH.2017.2654446, IEEE/ASME Transactions on Mechatronics

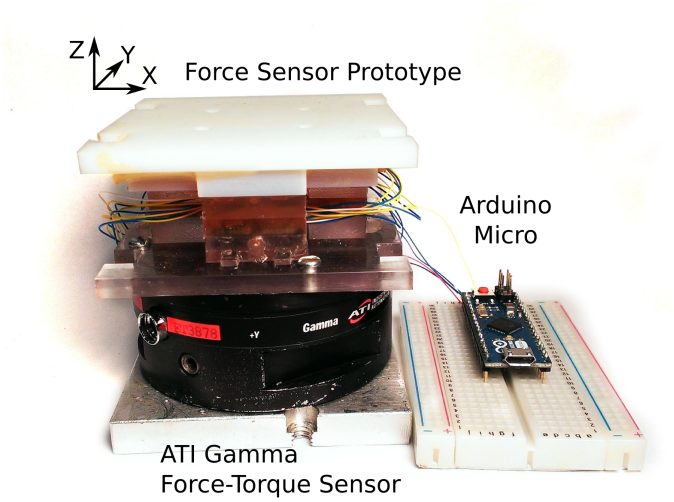

Fig. 7. The testing setup. The MEMS sensor was secured to a commercial force-torque sensor (ATI Gamma, ATI Automation). Loading was applied manually along all 6 axes. Data from the MEMS sensor was logged to a PC using an Arduino Micro.

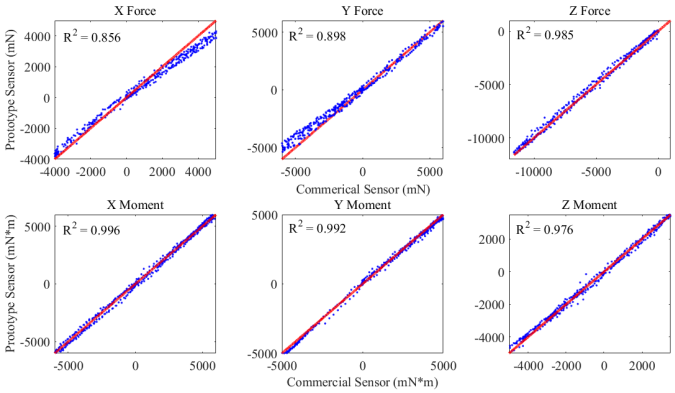

Fig. 8. Single direction loading for force and moment. The red line represents a perfectly matched response with the commercial force-torque sensor response while the blue dots are the actual response.

Torque sensor, ATI, Apex, North Carolina, USA). Uniaxial loading was achieved by fixing a string to the top plate and applying weights to the end of the string. Compound loading was achieved by grasping the top plate and manually manipulating the sensor through a range of different forces and moments to create a random time-varying compound input force. Data from the barometers was logged by an Arduino Micro and processed using Matlab (Fig. 7). Calibration used a first order least-squares fit with an affine term. Figure 8 shows the force-torque sensor response along all 6 axes against the commercial sensor. The blue dots represent a single time point and the red line represents the ideal, a one to one correspondence between the commercial sensor and the MEMS barometer sensor. Despite the low cost and simple fabrication, the sensor produces reasonably linear responses to single axis loading as demonstrated by the low RMS values.

Figure 9 represents the sensor response under compound loading. Finally, Figure 10 shows the MEMS sensor readings plotted alongside the commercial sensor readings during compound loading. The stiffness results for each axis are given in Table I.

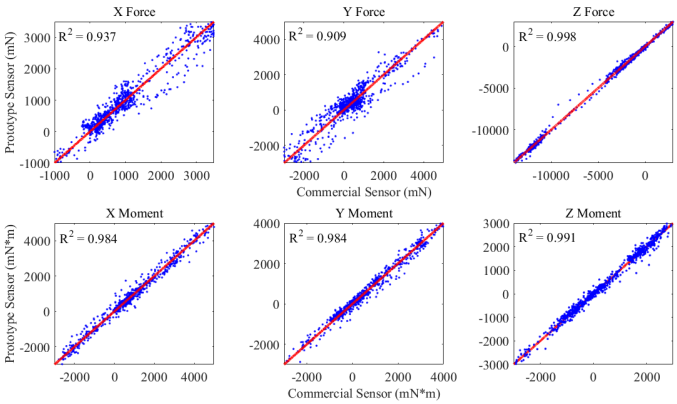

Fig. 9. Compound loading for (a) X Force (b) Y Force (c) Z Force (d) X Moment (e) Y Moment (f) Z Moment. The red line represents a perfectly matched response with the commercial force-torque sensor response while the blue dots are the actual response.

TABLE I
STIFFNESS OF THE MEMS FORCE-TORQUE SENSOR

AXIS	STIFFNESS
FX	26.4 N/mm
FY	27.4 N/mm
FZ	193 N/mm
MX	7.06 N/degree
MY	7.55 N/degree
MZ	3.93 N/degree

The RMS error was also calculated during an unloaded condition in order to determine the noise of the MEMS sensor. These values are given in Table II.

IV. DISCUSSION

A. Discussion

This paper presents a simple design that demonstrates MEMS barometers can be used to create a six-axis force-torque sensor at low-cost. The total cost of components is under twenty dollars, including the barometer chips, microcontrollers, printed circuit boards, urethane rubber (Vytaflex 20), and rigid plastic for top and bottom mounting plates. The barometers are assumed to be mounted on a single flat PCB in keeping with the design goal of a low-cost, easily-manufactured system. The circuit boards and casting process are all compatible with commodity mass-production techniques. This contrasts with current standard approach of cutting flexures from metal (typically using electric discharge

TABLE II
NOISE OF THE MEMS FORCE-TORQUE SENSOR

AXIS	NOISE
FX	22.0 mN
FY	18.7 mN
FZ	22.5 mN
MX	16.7 mN*m
MY	18.5 mN*m
MZ	4.43 mN*m

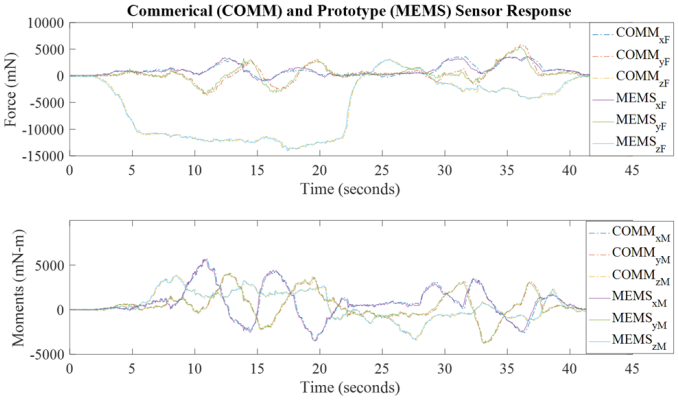

Fig. 10. Commercial force-torque sensor alongside MEMS force torque sensor during typical compound loading.

machining) and bonding strain gauges to them, an expensive procedure.

During single-axis loading experiments, the MEMS sensor was loaded past 10N with an R^2 greater than 0.97 for F_z, M_x, M_y, and M_z and an R^2 greater than 0.85 for F_x and F_y. The error for F_x and F_y is larger at the extremes of the loading range, suggesting the working range is smaller for these axes as compared to the other axes. The MEMS sensors were loaded up to 5N - 12N during compound loading with an R^2 greater than 0.90 for F_x and F_y and an R^2 greater than 0.98 for F_z, M_x, M_y, and M_z. The higher error in F_x and F_y is likely due to cross-talk between these axes and others during compound loading and the sensors flexing along these axes during loading. This last issue could be solved by stiffening the sensor along these axes. In fact, due to the nature of the design of this sensor, many design parameters exist that can be independently modified to tune the force sensitivity and force range of the sensor based on need. Preliminary prototypes with uninstrumented rubber blocks in parallel have improved the range to hundreds of Newtons for single-DOF units. An optimal design, including variations in materials and geometries, is deferred to future work. Thermal variations do impact the sensor, but they can be compensated down to within 5 counts.

The proposed force-torque sensor has advantages over force-torque sensors currently in use in a number of applications. For example, force-torque sensors are currently used in robot fingers to measure contact location and contact force while other sensors are mounted to the wrist of robot arms to improve manipulation in unstructured environments [14]. Commercial force sensors, though highly accurate with errors smaller than 0.05%, are expensive and susceptible to overload damage thus limiting their use for these applications [15]. With a bandwidth above 50 Hz, our sensor is a robust and low-cost alternative, allowing it to be deployed more readily for use where unexpected collisions are likely. Further, our sensor outperforms other low-cost sensors, particularly for the F_z, M_x, M_y, and M_z axes. The FSR-based design described by Rikker et al. [9] showed errors up to 2.9% for single axis loading. Similarly, a 6-axis force torque sensor using piezoresistive load-sensing bridges showed errors for single-axis loading between 3% and 4% for loads in F_x, F_y, and F_z and errors between 5% and 10% for loads in M_z [16]. Finally, the fabrication of our sensor requires only off-the-shelf components, making it both easily translatable to other labs and customizable to a specific application.

B. Conclusion

This paper outlined the design of a 6DOF force torque sensor from barometric sensors. The design is easy to fabricate, low-cost, and robust. This provides useful behavior in a niche that is unmet by current six-axis force-torque sensors based on strain-gauges, as it is significantly lower cost and better able to withstand high loads without failure. The sensors could be further optimized to improve performance, and the simple design lends itself to easy customization for different applications. Both the sensitivity and the physical size of the sensor can be tailored by choice of materials and variations in the geometry of the sensor.

ACKNOWLEDGMENTS

This work was supported by the National Science Foundation under Award No. IIS-0905180 and by the Defense Advanced Research Agency under Contract No. W91CRB-10-C-0141.

REFERENCES

[1] R. R. J. P. D. H.J. Pandya, Hyun Tae Kim, "Mems based low cost piezoresistive microcantilever force sensor and sensor module," *Materials Science in Semiconductor Processing*, vol. 19, pp. 163–173, 2014.

[2] C. Kang, "Performance improvement of a 6-axis force-torque sensor via novel electronics and cross-shaped double-hole structure," *International Journal of Control and Automation Systems*, vol. 3, no. 3, p. 469, 2005.

[3] Y.-J. Li, J. Zhang, Z.-Y. Jia, M. Qian, and H. Li, "Research on force-sensing element's spatial arrangement of piezoelectric six-component force/torque sensor," *Mechanical Systems and Signal Processing*, vol. 23, no. 8, pp. 2687 – 2698, 2009. [Online]. Available: http://www.sciencedirect.com/science/article/pii/S0888327009001514

[4] A. F. Fernandez, F. Berghmans, B. Brichard, P. Mgret, M. Decrton, M. Blondel, and A. Delchambre, "Multi-component force sensor based on multiplexed fibre bragg grating strain sensors," *Measurement Science and Technology*, vol. 12, no. 7, p. 810, 2001. [Online]. Available: http://stacks.iop.org/0957-0233/12/i=7/a=310

[5] Y.-L. Park, S. C. Ryu, R. Black, K. Chau, B. Moslehi, and M. Cutkosky, "Exoskeletal force-sensing end-effectors with embedded optical fiber-bragg-grating sensors," *Robotics, IEEE Transactions on*, vol. 25, no. 6, pp. 1319–1331, 2009.

[6] F. Beyeler, S. Muntwyler, and B. J. Nelson, "Design and calibration of a microfabricated 6-axis force-torque sensor for microrobotic applications," in *Robotics and Automation, 2009. ICRA'09. IEEE International Conference on*. IEEE, 2009, pp. 520–525.

[7] F. Beyeler, S. Muntwyler, and B. J. Nelson, "A six-axis mems force–torque sensor with micro-newton and nano-newtonmeter resolution," *Microelectromechanical Systems, Journal of*, vol. 18, no. 2, pp. 433–441, 2009.

[8] P. Berkelman, L. Whitcomb, R. Taylor, and P. Jensen, "A miniature microsurgical instrument tip force sensor for enhanced force feedback during robot-assisted manipulation," *Robotics and Automation, IEEE Transactions on*, vol. 19, no. 5, pp. 917–921, 2003.

[9] J. Rikkers, "Design of a miniature low-budget torque sensor," Technical Report 015CE2008, University of Twente, Tech. Rep., 2008.

[10] G. Hirzinger, J. Bals, M. Otter, and J. Stelter, "The dlr-kuka success story: robotics research improves industrial robots," *Robotics Automation Magazine, IEEE*, vol. 12, no. 3, pp. 16–23, 2005.

[11] (2013) The spacemouse family of 3d interface devices. [Online]. Available: http://www.3dconnexion.com/products

[12] Y. Tenzer, L. P. Jentoft, and R. D. Howe, "Inexpensive and easily customized tactile array sensors using mems barometers chips," 2014. *Robotics Automation Magazine, IEEE*, vol. 21, no. 3, 2014.
[13] C. Reeks, M. G. Carmichael, D. Liu, and K. J. Waldron, "Angled sensor configuration capable of measuring tri-axial forces for phri," *International Conference on Robotics and Automation*, 2016.
[14] A. Bicchi, J. K. Salisbury, and D. L. Brock, "Contact sensing from force measurements," *The International Journal of Robotics Research*, vol. 12, no. 3, pp. 249–262, 1993.
[15] (2014) Honeywell Torque Sensors Product Range Guide. [Online]. Available: http://sensing.honeywell.com/honeywell-test-measurement-torque-range-guide-008897-1-en.pdf
[16] C. Jacq, B. Luthi, T. Maeder, O. Lambercy, R. Gassert, and P. Ryser, "Thick-fil multi-DOF force-torque sensor for wrist rehabilitation," *Sens. Actuators A Phys.*, vol. 162, no. 2, pp. 361–366, 2010.

Jacob Guggenheim Jacob W. Guggenheim is a PhD Student at the D'arbeloff Lab working under Professor Harry Asada in the Mechanical Engineering at Massachusetts Institute of Technology. He received his B.S in Bioengineering from the University of Illinois, Urbana-Champaign. His research interests focus on developing automated tools for biology research.

Leif P. Jentoft is a co-founder of RightHand Robotics, and TakkTile LLC. He did his doctoral studies at the Biorobotics Lab at the Harvard School of Engineering and Applied Science, and received his B.S. in Engineering from Olin College in 2009 where he studied robotics and systems engineering. His research interests focus on grasping, tactile sensing, passive mechanics, and low-cost robots for unstructured tasks.

Yaroslav Tenzer is a co-founder of RightHand Robotics (RHR) and TakkTile LLC. He was a post-doctoral researcher at the Biorobotics laboratory at Harvard University. Dr. Tenzer received a PhD in Medical Robotics from the Department of Mechanical Engineering at Imperial College London, UK. The Bachelor in Mechanical Engineering and the Masters degree in Mechatronics he received from Ben-Gurion University, Israel.

Robert D. Howe is the Abbott and James Lawrence Professor of Engineering and Area Dean for Bioengineering in the Harvard School of Engineering and Applied Sciences. He earned a bachelors degree in physics from Reed College, then worked in the electronics industry in Silicon Valley. He received a doctoral degree in mechanical engineering from Stanford University, then joined the faculty at Harvard in 1990. He directs the Harvard BioRobotics Laboratory, which investigates the roles of sensing and mechanical design in motor control, in both humans and robots. His research interests focus on manipulation, the sense of touch, haptic interfaces, and robot-assisted and image-guided surgery